

## High-Speed Electroseparations Inside Silica Colloidal Crystals

Suping Zheng, Eric Ross, Michael A. Legg, and Mary J. Wirth\*

Department of Chemistry, University of Arizona, 1306 East University Boulevard, Tucson, Arizona 85721

Received April 17, 2006; Revised Manuscript Received May 23, 2006; E-mail: mwirth@email.arizona.edu

Colloidal crystals have attracted intense interest as photonic materials,<sup>1</sup> chemical sensors,<sup>2</sup> perm-selective modifiers for electrodes,<sup>3</sup> and porous supports for lipid bilayers.<sup>4</sup> Here we report their use as a medium for chemical separations.<sup>5</sup> They exhibit fast mass transport. They have the ability to withstand high electric fields, and their surfaces can be chemically modified in the same way as silica gel. We demonstrate the separation of three cationic, hydrophobic dyes in 6 s over a separation length of 1 mm, using a C<sub>18</sub> stationary phase and a field strength of 1000 V/cm. We also demonstrate the separation of three peptides in 10 s over a 6 mm separation length. The results reveal marked improvement in peak width over chromatographic monoliths.

There is a demand for much higher speed and miniaturization in separations. Capillary electrophoresis can be performed in very fast<sup>6,7</sup> time scales, but the separations lack high selectivity. Reversed-phase HPLC is more selective, but it is slower than electrophoresis because the flow rate, to maintain equilibrium, cannot exceed the rate of analyte diffusion between mobile and stationary phases. Faster HPLC is achieved using smaller (<2 μm), nonporous particles,<sup>8</sup> but this requires ultrahigh pressure and long column lengths due to the low surface areas. Monoliths of either silica<sup>9,10</sup> or polymer<sup>11</sup> offer smaller diffusion distances to increase separation speed without sacrificing surface area or requiring high pressures. In this work, crystals of nonporous, 200 nm colloids are studied as media that offer high surface area and even smaller dimensions for analyte diffusion in the mobile phase. Their performance is compared with a commercial silica monolith.

A 20 μm thick crystal was made of 200 nm diameter silica colloids by vertical deposition onto a fused silica slide.<sup>1</sup> Colloids were calcinated at 600 °C before deposition.<sup>12</sup> The crystal was hardened by sintering at 900 °C and then rehydroxylated to regenerate the surface silanol groups.<sup>13</sup> The material was silylated with ClSi(CH<sub>3</sub>)<sub>2</sub>(CH<sub>2</sub>)<sub>17</sub>CH<sub>3</sub>, then endcapped with ClSi(CH<sub>3</sub>)<sub>3</sub>. The resulting medium should have negligible electro-osmotic flow. A 1.5 cm × 2 mm strip of this material was assembled into a device depicted in Figure 1, which was used for separations.<sup>14</sup>

Three structurally similar dyes, DiIC12, DiIC16, and DiIC18, were used as analytes. These have the same singly charged headgroup, but differ in the lengths of their dual hydrocarbon chains. Electrokinetic injection was used: the dye mixture was put into the reservoir, 50 V/cm was applied for 5 s, then the voltage was turned off and the sample replaced with mobile phase. This differs from electrochromatography<sup>15</sup> in that there is no flow. Figure 2a shows the separation of the three DiIs. Peaks for the three components are baseline-resolved in the 1 mm separation length in 6 s, using a field strength of 1000 V/cm. A priori, the separation can occur either by electrophoresis or by differential adsorption. It can readily be shown<sup>14</sup> that the migration velocity,  $v_m$ , has contributions from both electrophoretic mobility,  $\mu_e$ , and

$$v_m = \mu_e E / (1 + k') \quad (1)$$

the reversed-phase capacity factor,  $k'$ , where  $E$  is the field. The

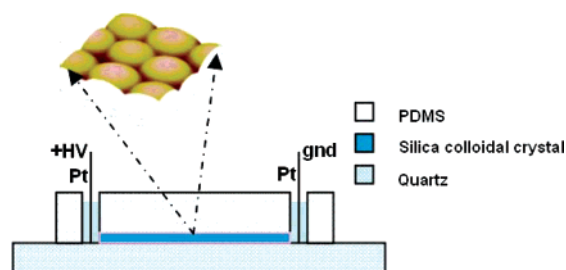


**Figure 1.** Schematic. The crystal was covered tightly with a 5 mm thick PDMS sheet, into which holes for reservoirs were cut. The insert is an AFM image of the 200 nm silica spheres. An inverted fluorescence microscope monitored the migration of the dyes. Details are provided.<sup>14</sup>

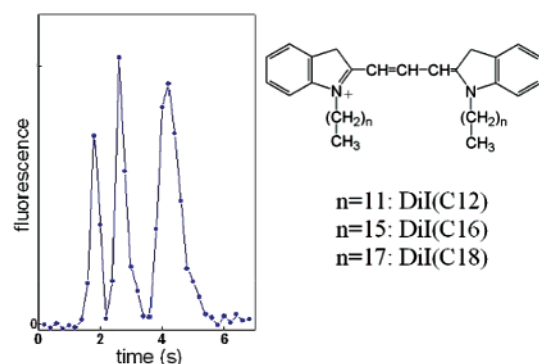


**Figure 2.** Separation of three DiIs through 1 mm of colloidal crystal using 90:10 MeOH:water, 0.1% TFA, and a field strength of 1000 V/cm.

electrophoretic mobilities of the three DiIs, measured in this mobile phase by capillary electrophoresis, are  $4.7 \times 10^{-6} \text{ cm}^2/(\text{V}\cdot\text{s})$  for DiIC12 and  $4.4 \times 10^{-6} \text{ cm}^2/(\text{V}\cdot\text{s})$  for DiIC16 and DiIC18. The small differences in electrophoretic mobility are not enough to account for the large differences in migration times, therefore, we conclude that the resolution is mainly achieved through reversed-phase adsorption.

An important figure of merit in evaluating a new medium for separations is the peak variance,  $\sigma^2$ , normalized for column length,  $L$ , which is referred to as the plate height,  $H$ . Smaller  $H$  indicates a better medium. Equation 2 gives a simple relation between plate height and separation velocity,  $v$ , which is the van Deemter

$$H = A + C \times v \quad (2)$$

equation for moderate to high velocities. The term  $A$  is a measure of the uniformity of the medium. A heterogeneously packed medium would give different path lengths to increase peak variance. The colloidal crystal is expected to have exceptional uniformity since it is a crystal. The  $C$  term is a measure of how slow the mass transport is through the medium, including diffusion through the mobile phase to reach the stationary phase. The colloidal crystal is expected to have much faster mass transport because the particles are 10-fold smaller than those used in HPLC.

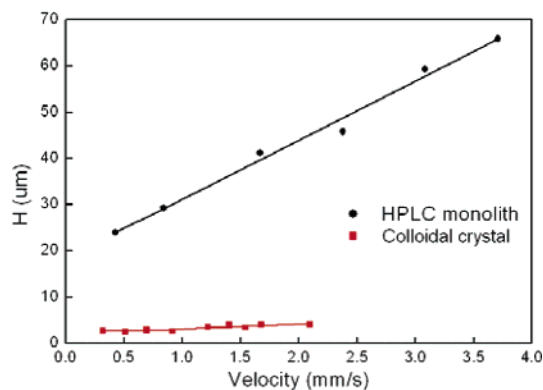


**Figure 3.** van Deemter plots for Merck Chromolith ( $\nu$ ) and the colloidal crystal ( $\gamma$ ). The same mobile phase was used as for Figure 2.

A van Deemter plot for DiIC12 in the colloidal crystal is shown in Figure 3. For comparison, the van Deemter plot is shown for a commercial monolithic column, Merck Chromolith, which has a 2.5 cm length and the same chemically modified surface. For the colloidal crystal, the van Deemter plot uses the velocity of an unretained dye, Rhodamine 6G, since there is no flow. This dye marker elutes with the system peak in HPLC, and in the separation of Figure 2, this dye would elute at 0.9 s.<sup>14</sup>

The van Deemter plots for the two materials differ markedly, with the colloidal crystal exhibiting much smaller, more favorable plate heights at all velocities. The  $A$  term for the colloidal crystal is 2.4  $\mu\text{m}$ , while  $A = 19 \mu\text{m}$  for the Merck Chromolith. The injected width contributes negligibly in both cases.<sup>12</sup> The  $C$  term is also remarkably smaller for the colloidal crystal: 1.2 ms for the colloidal crystal versus 12.8 ms for the Merck Chromolith. The size of the  $C$  term limits the speed of separations, and the much lower  $C$  term for the colloidal crystal is thus significant for the potential use of colloidal crystals in fast separations. The colloidal crystal thus achieves the expected large decreases in both  $A$  and  $C$  to give much lower peak variance than the high quality HPLC monolith.

As mentioned earlier, both adsorption and electrophoresis contribute to migration rate, as was shown by eq 1. This dual selectivity could be advantageous for peptide separations, where small, hydrophilic peptides coelute in HPLC. Figure 4 shows a separation of a mixture of three peptides, each labeled with Rhodamine dye, in 90:10 MeOH:water and 0.1% TFA. The peptide sequences are also given in Figure 4, written left-to-right from the N- to C-terminus and indicating the end bearing the rhodamine label (Rh). Peptides 1 and 2 each has a +2 charge, while peptide 3 has a +1 charge. The three peptides are shown to coelute in HPLC at 1 mL/min (Figure 4a). The tail in the chromatogram of Figure 4a is from peptide 3 eluting slightly later than peptides 1 and 2. The three peptides are shown to be well resolved by the colloidal crystal in less than 10 s at 800 V/cm (Figure 4b). The elution times track the electrophoretic mobilities.<sup>9</sup> A separation length of 6 mm was used for the colloidal crystal. The low peak variance per length is consistent with the van Deemter plot of Figure 3.

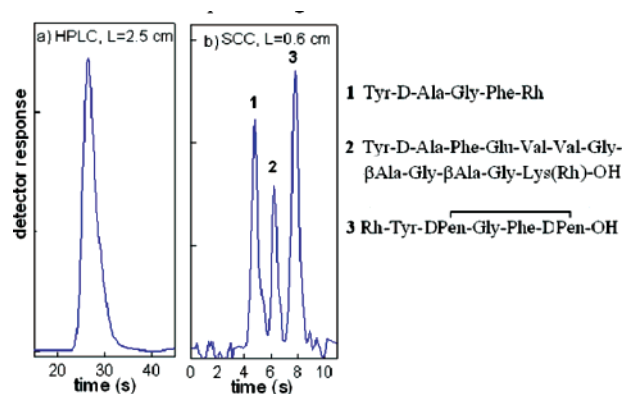


**Figure 4.** Separation by (a) HPLC and (b) the silica colloidal crystal of three peptides whose structures are shown to the right. The same mobile phase as in Figure 2 was used for both separations.

This work reports the first use of colloidal crystals for chemical separations. The results reveal that electrically driven transport achieves highly efficient separation of charged analytes. A separation based on differences in adsorptivity is demonstrated in Figure 1, and a separation based on differences in electrophoretic mobility is demonstrated in Figure 4. The results show greatly reduced peak width and greatly increased speed of mass transport compared to the commercial monolithic stationary phase. The short distance of 1 mm for a reversed-phase separation is unprecedented.

**Acknowledgment.** This work was supported by the National Institutes of Health under Grant 1 R01 GM65980.

**Supporting Information Available:** Details about the colloidal crystals, the device and the separations, and a more complete reference list are available. This material is available free of charge via the Internet at <http://pubs.acs.org>.

## References

- (1) (a) Bogush, G. H.; Tracy, M. A.; Zukoski, C. F. J., IV. *Non-Crystalline Solids* **1988**, *104*, 95. (b) Jiang, P.; Bertone, J. F.; Hwang, K. S.; Colvin, V. L. *Chem. Mater.* **1999**, *11*, 2132. (c) Im, S. H.; Kim, M. H.; Park, O. O. *Chem. Mater.* **2003**, *15*, 1797.
- (2) Goponenko, A. V.; Asher, S. A. *J. Am. Chem. Soc.* **2005**, *127*, 10753.
- (3) Newton, M. R.; Bohaty, A. K.; White, H. S.; Zharov, I. *J. Am. Chem. Soc.* **2005**, *127*, 7268.
- (4) Brozell, A. M.; Muha, M. A.; Sanii, B.; Parikh, A. N. *J. Am. Chem. Soc.* **2006**, *128*, 62.
- (5) A patent application has been filed.
- (6) Jacobson, S. C.; Culbertson, C. T.; Daler, J. E.; Ramsey, J. M. *Anal. Chem.* **1998**, *70*, 3476.
- (7) Plenert, M. L.; Shear, J. B. *Proc. Natl. Acad. Sci. U.S.A.* **2003**, *100*, 3853.
- (8) MacNair, J. E.; Patel, K. D.; Jorgenson, J. W. *Anal. Chem.* **1999**, *71*, 700.
- (9) Leinweber, F. C.; Lubda, D.; Cabrera, K.; Tallarek, U. *Anal. Chem.* **2002**, *74*, 2470.
- (10) Luo, Q.; Shen, Y.; Hixson, K. K.; Zhao, R.; Yang, F.; Moore, R. J.; Mottaz, H. M.; Smith, R. D. *Anal. Chem.* **2005**, *77*, 5028.
- (11) Xie, S.; Allington, R. W.; Svec, F.; Fréchet, J. M. J. *J. Chromatogr. A* **1999**, *865*, 169.
- (12) Chubanov, A. A.; Jun, Y.; Norris, D. J. *Appl. Phys. Lett.* **2004**, *84*, 3573.
- (13) Köhler, J.; Kirkland, J. J. *J. Chromatogr.* **1987**, *385*, 125.
- (14) See Supporting Information.
- (15) Vegavri, A.; Guttman, A. *Electrophoresis* **2006**, *27*, 716.

JA062676L